# Ga-NMR local susceptibility of the Kagome-based magnet $SrCr_{9p}Ga_{12-9p}O_{19}$: A high-temperature study

**L. Limot, P. Mendels, G. Collin, C. Mondelli, H. Mutka, and N. Blanchard**

**Abstract**: We report a high-$T$ Ga–NMR study in the Kagome-based anti-ferromagnetic compound $SrCr_{9p}Ga_{12-9p}O_{19}$ ($0.81 \leq p \leq 0.96$), and present a refined mean-field analysis of the local NMR susceptibility of Cr-frustrated moments. We find that the intralayer Kagome coupling is $J = 86(6)$ K, and the interlayer coupling to non-Kagome Cr moments is $J' = 69(7)$ K. The $J'/J = 0.80(1)$ ratio confirms the common belief that the frustrated entity is a pyrochlore slab.

PACS Nos.:75.30Cr, 75.50Lk, 76.60-k

**Résumé** : Nous présentons des mesures RMN à haute température sur du Ga dans le composé antiferromagnétique $SrCr_{9p}Ga_{12-9p}O_{19}$ basé sur un réseau de Kagomé ($0{,}81 \leq p \leq 0{,}96$) et proposons une analyse en champ moyen améliorée de la susceptibilité RMN des moments frustrés du Cr. Nous trouvons que le couplage intra-couche de Kagomé est $J = 86(6)$ K et que le couplage inter-couches aux moments des ions Cr non Kagomé est $J' = 69(7)$ K. Le rapport $J'/J = 0{,}80(1)$ confirme ce qui est généralement accepté que l'entité frustrée est une couche pyrochlore.

[Traduit par la Rédaction]

The Kagome-based compound $SrCr_{9p}Ga_{12-9p}O_{19}$[SCGO($p$), $p < 1$] has been receiving considerable attention as a model system for geometrically frustrated physics [1]. Magnetic properties of SCGO($p$) arise from Heisenberg $Cr^{3+}$ ions ($S = \frac{3}{2}$). Despite macroscopic susceptibility ($\chi_{\text{macro}}$) measurements that indicate that a strong anti-ferromagnetic interaction couples neighboring spins ($\Theta_{\text{macro}} \approx 500$–600 K), the spin–spin correlation length never exceeds twice the Cr–Cr distance [2]. No classical Néel long-range order occurs. On the contrary, SCGO($p$) continues to display Curie–Weiss behavior well below $\Theta_{\text{macro}}$ as suggested by the linear $T$-dependence of $\chi^{-1}_{\text{macro}}$, extending mean-field predictions to an unusual temperature domain ($T << \Theta_{\text{macro}}$).

Received June 12, 2000. Accepted August 8, 2001. Published on the NRC Research Press Web site on December 5, 2001.

**L. Limot,[1] P. Mendels, and N. Blanchard.** Laboratoire de Physique des Solides, UMR 8502, Université de Paris-Sud, 91405 Orsay, France.
**G. Collin.** Laboratoire Léon Brillouin, CE Saclay, CEA-CNRS, 91191 Gif-sur-Yvette, France.
**C. Mondelli and H. Mutka.** Institut Laue-Langevin, B.P. 156, F-38042 Grenoble Cedex 9, France.

[1] Corresponding author .

 DOI: 10.1139/cjp-79-11/12-1393 

Geometric frustration arises from interacting spins on Kagome networks. However, the crystal structure is not pure Kagome since $Cr^{3+}$ ions occupy both Kagome [Cr(12$k$)] and non-Kagome [Cr(2$a$),Cr(4$f_{vi}$)] sites, as shown in the inset of Fig. 1. Cr(2$a$) sites link two Kagome layers. The Kagome-Cr(2$a$)–Kagome slabs are isolated from one another by Cr(4$f_{vi}$)−Cr(4$f_{vi}$) pairs that Lee et al. showed to form spin singlets with a binding energy of $\Delta = 216$ K [3]. They also suggested that the Kagome-Cr(2$a$)–Kagome slab may be regarded as a quasi-2D highly frustrated system, which they named pyrochlore slab. However, there is a lack of experimental evidence concerning couplings that ensure this slab structure. Coupling of the two Kagome planes through Cr(2$a$) is not known, nor is the intralayer Kagome coupling. One way to shed light on this problem, would be a refined high-$T$ analysis of the magnetic susceptibility of Cr-frustrated moments. Unfortunately, this is prevented in $\chi_{\text{macro}}$ by the fact that there are contributions from all magnetic sites, frustrated and nonfrustrated. Moreover, $\chi_{\text{macro}}$ is also sensitive to disorder as nonmagnetic $Ga^{3+}$ ions are always present on $Cr^{3+}$ sites (the $p = 1$ compound is not stable) [4]. As we show here, such an analysis can be done by $^{69}$Ga and $^{71}$Ga ($I = \frac{3}{2}$) NMR since Ga nuclei on site 4$f$ directly probe both Cr(12$k$) and Cr(2$a$) moments (see, inset Fig.1). By varying Ga/Cr substitution from 4% to 19% ($p = 0.81$, 0.89, and 0.96), we are able to separate and identify on a firm experimental ground the substitution-related susceptibility from the intrinsic frustrated susceptibility of the slab [5].[2] We present here high-$T$ results and mean-field analysis of the slab susceptibility, which enables us to evaluate $J'$ and $J$, respectively, the Cr(2$a$)−Cr(12$k$) coupling and the Cr(12$k$)−Cr(12$k$) coupling. We find $J' = 69(7)$ K and $J = 86(6)$ K. The $J'/J = 0.80(1)$ ratio confirms the common belief that the frustrated entity is a pyrochlore slab.

All samples are ceramics and were synthesized by solid-state reaction as detailed elsewhere.[1] Reaction products were checked by standard X-ray diffraction and refined by neutron diffraction (see Table 1). $\chi_{\text{macro}}$ yielded results in agreement with previous concentrations reported in the literature ($\Theta_{\text{macro}} = 439(22)$, 501(14), and 608(14) K for $p = 0.81$, 0.89, 0.96, respectively) [6].

An extended NMR analysis of the spectrum was presented in previous papers [7].[1] Three different Ga NMR sites can be resolved: Ga(4$e$), Ga(4$f$), and Ga substituted on Cr sites [Ga(sub.)]. Ga(4$f$) is at the heart of the frustrated physics in SCGO (inset Fig. 1). It is exclusively coupled to Cr(12$k$) and Cr(2$a$) through a Ga–O–Cr hyperfine interaction, and is the object of the present study.

A set of spectra ranging from 150 to 410 K were recorded in a ∼7 T permanent magnet. We used a $\pi/2, \pi$ sequence with spacing $\tau = 18$ $\mu$s between pulses, and as the applied frequency was swept over a ∼1 MHz range, with a step interval of 75 kHz, spin-echo signals were recorded. The overall spectrum was then obtained by summing all the spin-echo Fourier transforms [8]. Another set of spectra ranging from 15 to 200 K were obtained in a sweep field setup, i.e., by varying an external magnetic field at a constant applied frequency 40.454 MHz, and recording the integral of the spin-echo signal. Again, we used a conventional $\pi/2, \pi$ sequence, but with spacing $\tau = 28$ $\mu$s.

A typical set of high-$T$ ($T \geq 100$ K) field sweep spectra for the $p = 0.96$ sample, recorded around 3 T, is reported in Fig. 1. In this field window, two lines are unambiguously resolved. Ga(4$f$) is the main line and the hump at its right is Ga(sub.). The negligible contribution of Ga(sub.) to the spectrum reflects the nearly stoichiometric composition of the sample. The sharp nonsymmetric features of the Ga(4$f$) line originate from $T$-independent quadrupole effects ($^{71}\nu_Q(4f) \simeq 2.9$ MHz, $\eta \simeq 0$) related to the local charge environment around the nucleus. Upon cooling the NMR line shifts towards lower fields, without any appreciable broadening. The $T$-dependence of the shift ($K$) stems from the Ga(4$f$) magnetic environment. $K$ provides a direct measurement of the magnetic susceptibility of the Cr(12$k$) and Cr(2$a$) ions (to be detailed below).

The temperature dependence of $K^{-1}$ is presented in Fig. 2 for all samples. The high-$T$ data ($T \gtrsim 100$ K) follows a Curie–Weiss law as suggested by the linear variation of $K^{-1}$. By extrapolating $K^{-1}$ to 0 we extract the NMR Curie–Weiss temperature ($\Theta_{\text{NMR}}$). We evaluate it to be 453(50), 469(44),

[2] L. Limot, P. Mendels, G. Collin, C. Mondelli, H. Mutka, N. Blanchard, and M. Mekata. Manuscript in preparation.

**Fig. 1.** Typical $^{71}$Ga field sweep obtained at 40.454 MHz for $p = 0.96$. From right to left: 150, 120, and 100 K. The zero-shift reference position is 3.116 T. The horizontal arrow indicates the shift direction upon cooling. Inset: crystal structure of ideal $SrCr_9Ga_3O_{19}$. The thick broken lines show the hyperfine coupling paths of Ga($4f$) nucleus to frustrated Cr moments. Light grey circles are oxygen. Cr($12k$) are arranged to form a distorted Kagome network and are coupled through Cr($2a$). The full structure is Cr($4f_{vi}$)−Cr($4f_{vi}$)/Kagome–Cr($2a$)–Kagome/Cr($4f_{vi}$)−Cr($4f_{vi}$), etc.

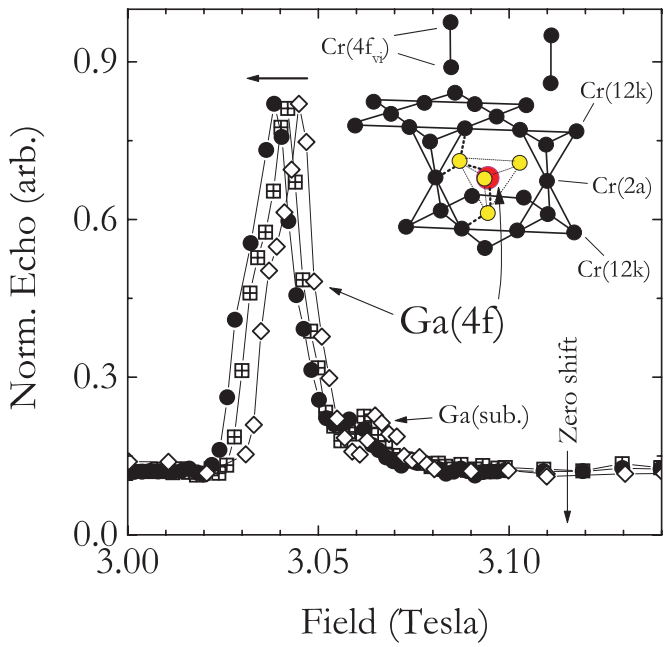


and 484(40) K for $p = 0.84$, 0.89, and 0.96, respectively, of the same order of $\Theta_{\text{macro}}$, but somewhat lower. The increase in $\Theta_{\text{NMR}}$ with $p$ reflects a better lattice coverage as one would expect from mean-field theory. Here again Curie–Weiss behavior extends well below $\Theta_{\text{NMR}}$. If $T$ is lowered further, $K$, in all samples, eventually deviates from Curie–Weiss behavior, flattening and even decreasing below $T = 40$–$50$ K. We refer the reader to other publications for a detailed discussion on the low-$T$ behavior of $K$ [5].[1]

We now turn to a discussion of the high-$T$ behavior of $K$ within a mean-field analysis. First, we would like to point out that Cr($12k$) and Cr($2a$) do not have the same magnetic environment. Cr($2a$) has six nearest neighbors of Cr($12k$), whereas Cr($12k$) has five nearest neighbors (four Cr($12k$) and one Cr ($2a$)). Furthermore, the Cr($12k$)–Cr($12k$) coupling ($J$) and the Cr($12k$)–Cr($2a$) coupling ($J'$) are a priori not the same. In this regard our mean-field analysis is similar to that performed in ferrimagnetic compounds, which bear inequivalent magnetic sites.

To justify this analysis, we must argue how $J$ and $J'$ are the only relevant couplings in the slab. A study of a series of chromium oxides indicates that the Cr–Cr interaction is dominated by direct exchange [9]. It was shown that such an interaction varies rapidly with Cr–Cr distance (and Cr–O–Cr angle), being $\approx 0$ when $d_{\text{Cr-Cr}} \gtrsim 3.1$ Å. Therefore, only interactions between Cr($12k$)–Cr($12k$) ($d_{\text{Cr-Cr}} = 2.895$ Å) and Cr($12k$)–Cr($2a$) ($d_{\text{Cr-Cr}} = 2.971$ Å) are relevant in the frustrated unit, with $0 < J' < J$. The Cr($2a$)–Cr($2a$) interaction is $\approx 0$ as $d_{\text{Cr-Cr}} = 5.80$ Å. Note that the Kagome layer is distorted, therefore $J$ represents the average coupling between Cr($12k$).

On the basis of these considerations, the frustrated spin Hamiltonian is

$$\mathcal{H} = J \sum_{\langle i,j \rangle} \left[ (\vec{S}_{12k})_i \cdot (\vec{S}_{12k})_j + \varepsilon (\vec{S}_{12k})_i \cdot (\vec{S}_{2a})_j \right]$$

**Fig. 2.** $K^{-1}$ versus $T$ down to 15 K, for all samples. Minor second-order quadrupole corrections have been performed. The straight line extrapolation of $K^{-1} = 0$ yields $\Theta_{\mathrm{NMR}}$.

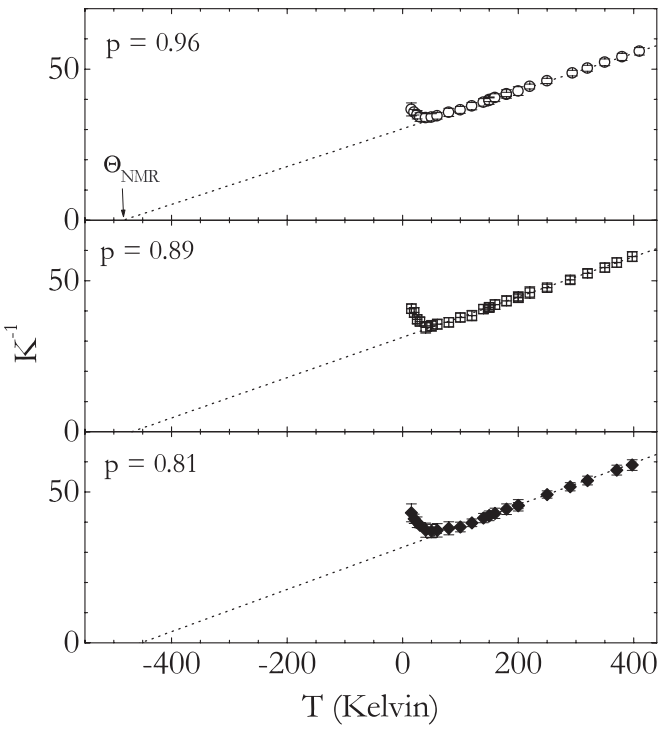


where we have introduced $0 < \varepsilon = J'/J < 1$. The first term is the isotropic Heisenberg interaction between spins $\vec{S}_{12k}$ on the Kagome layer. The second term is the interaction between $\vec{S}_{12k}$ and $\vec{S}_{2a}$ spins. The summation is taken over neighboring spins of the slab.

Using a mean-field approach, or a high-temperature expansion, the $\chi_{12k}$ and $\chi_{2a}$ susceptibilities per site of Cr($12k$) and Cr($2a$) can be written

$$\chi_{12k} = \frac{\mu_{\mathrm{eff}}^2}{3k_{\mathrm{B}}Tf(T)}\left(1 - \frac{p_{2a}S(S+1)\varepsilon J}{3k_{\mathrm{B}}T}\right) \tag{1}$$

and

$$\chi_{2a} = \frac{\mu_{\mathrm{eff}}^2}{3k_{\mathrm{B}}Tf(T)}\left(1 + \frac{6p_{12k}S(S+1)(2/3-\varepsilon)J}{3k_{\mathrm{B}}T}\right) \tag{2}$$

where $f(T) = 1 + 4p_{12k}S(S+1)J/3k_{\mathrm{B}}T - 6p_{12k}p_{2a}(\varepsilon JS(S+1)/3k_{\mathrm{B}}T)^2$. The two expressions are different and reflect the fact that the two sites have different magnetic environments. The effective magnetic moment is $\mu_{\mathrm{eff}} \approx 4\ \mu_{\mathrm{B}}$, typical of $S = 3/2$ $Cr^{3+}$ ions [10]. $p_{12k}$, $p_{2a}$ are the occupation of the Cr($12k$) and Cr($2a$) sites known from neutron refinement (cf. Table 1). The only unknown parameters are $J$ and $\varepsilon$. In Fig. 3, we show the evolution of $\chi_{12k}$ and $\chi_{2a}$ when increasing $\varepsilon$, with a fixed value $J$. In the limit $\varepsilon = 0$, $\chi_{12k}$ follows a Curie–Weiss law with a Kagome Curie–Weiss temperature $4p_{12k}JS(S+1)/3$, whereas $\chi_{2a}$ follows a Curie law, as we have freed the Cr($2a$) spin from its magnetic environment. As $\varepsilon$ is increased, the pure paramagnetic behavior of $\chi_{2a}$ progressively dies out, while $\chi_{12k}$ is little affected. Of interest is when the Kagome–Cr($2a$)–Kagome slab behaves as a pyrochlore slab. By pyrochlore slab, we mean that both magnetic sites are identical $\chi_{12k} = \chi_{2a}$,

**Fig. 3.** Calculated mean-field susceptibilities $\chi_{12k}$ and $\chi_{2a}$ of the Cr($12k$) and Cr($2a$) moments versus $T$, with increasing Cr($2a$)–Cr($12k$) coupling. $J$ is fixed at 85 K and $p_{12k} = p_{2a} = 1$.

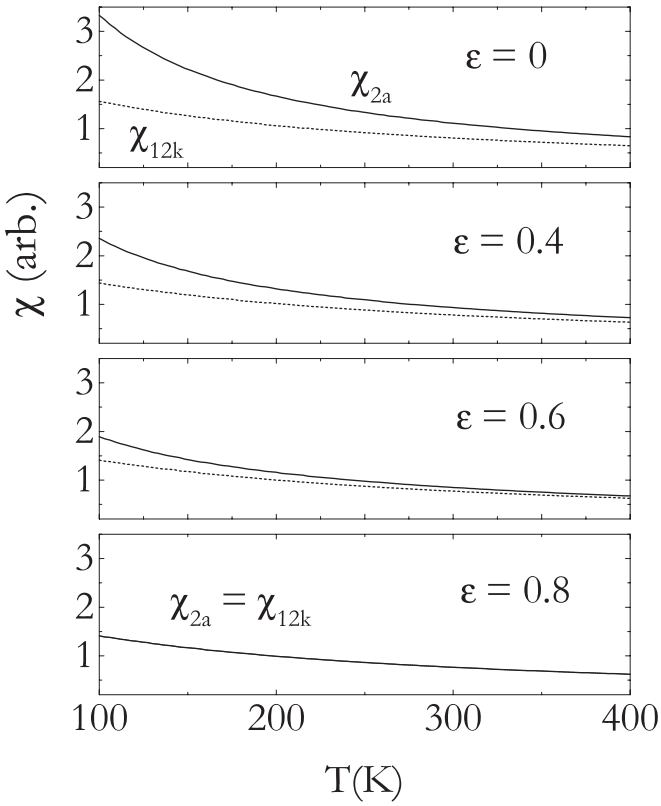


i.e., $\varepsilon = \varepsilon_0 = 4p_{12k}/(6p_{12k} - p_{2a})$. For an homogeneous substitution ($p_{12k} = p_{2a} = p$) $\varepsilon_0 = 0.8$, reflecting the fact that the effective exchange field on Cr($2a$) ($6J'$) and on Cr($12k$) ($4J + J'$) are then identical. We stress that this relation is independent on distortion on the Kagome layer, as it only involves the average exchange constant $J$.

We may express the NMR shift $K$ using the mean-field expressions (1) and (2)

$$K \propto (9\chi_{12k} + 3\delta\chi_{2a}) \tag{3}$$

where we have introduced $\delta = A'/A$. $A$, $A'$ are the hyperfine constants, which are, respectively, a measurement of the Cr($12k$), Cr($2a$) moment at the nuclear site, and just influence the thermal behavior of $K$ by their ratio $\delta$. The two terms of expression (3) are multiplied by the number of neighboring Cr($12k$) and Cr($2a$) linked by the oxygen ions to the Ga($4f$) nucleus, respectively, 9 and 3. We can fix a lower bound on $\delta$ by some simple structural remarks. The hyperfine bridge Ga($4f$)–O–Cr($12k$) yields bond lengths of $d_{\mathrm{Ga}(4f)-\mathrm{O}} = 1.866$ Å and $d_{\mathrm{O}-\mathrm{Cr}(12k)} = 2.052$ Å. The hyperfine bridge Ga($4f$)–O–Cr($2a$) yields bond lengths of $d_{\mathrm{Ga}(4f)-\mathrm{O}} = 1.866$ Å and $d_{\mathrm{O}-\mathrm{Cr}(2a)} = 1.971$ Å. The small difference in length and the similarity for angles between these bonds leads to a stronger coupling to Cr($2a$) than to Cr($12k$), and $\delta > 1$. A more precise calculation suggests $\delta \approx 2$ [7]. It is instructive to compare $K$ to the expression for the susceptibility of the Kagome–Cr($2a$)–Kagome slab that one would obtain from a macroscopic measurement

$$\chi_{\mathrm{slab}} = 6p_{12k}\chi_{12k} + p_{2a}\chi_{2a}$$

**Fig. 4.** The $(\varepsilon, J, \delta)$ set of values that reproduce the linear variation of $K^{-1}$ with $T$ of the $p = 0.96$ sample. For a given value of $\varepsilon$ (abscissa) there is an associated value $\delta$ (upper panel) and $J$ (bottom panel).

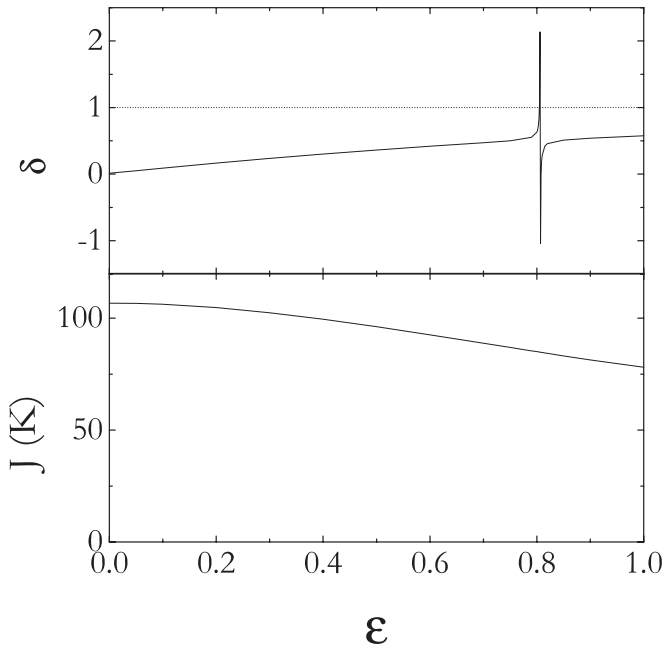


where $\chi_{12k}$ and $\chi_{2a}$ are now weighted by 6 and 1, respectively, the number of Cr($12k$) and Cr($2a$) per formula unit of SCGO. $K$ is an independent measurement of the slab susceptibility, but with a different weighting than $\chi_{\text{slab}}$. Using $\delta \approx 2$, we see that $\chi_{2a}$ and $\chi_{12k}$ impact $K$ in a ratio of 6/9 instead of 1/6 for $\chi_{\text{slab}}$. $K$, on the contrary, is very sensitive to the temperature dependence of $\chi_{2a}$, and this implies that it is also very sensitive to $\varepsilon$.

The shift $K$ reseals three unknown parameters $J$, $\varepsilon$, and $\delta$. Our aim is to determine their values by fitting for $T \geq 100$ K the shift data presented in Fig. 2. There are an infinity of $(\varepsilon, J, \delta)$ set of values that reproduce the linear variation of $K^{-1}$ with $T$. In Fig. 4, we present the set of $(\varepsilon, J, \delta)$ -values obtained when fitting $K^{-1}$ of the $p = 0.96$ sample to expression (3). As shown, for a given value of $\varepsilon$ (abscissa) there is an associated value $\delta$ (upper panel) and $J$ (bottom panel). To seize the evolution of this set of parameters, it is instructive to examine the dependence of $\delta$ on $\varepsilon$. In the limit $\varepsilon \to 0$, we see that $\delta \to 0$. In fact when $\varepsilon = 0$, $\chi_{2a}$ follows a Curie law. Therefore, to reproduce the linear variation of $K^{-1}$ there is only one possibility: uncouple the Ga($4f$) nuclei from Cr($2a$), setting $\delta = 0$. As $\varepsilon$ is increased, $\delta$ monotonically increases since the Curie contribution from $\chi_{2a}$ dies out. But when $\varepsilon = \varepsilon_0$ expression (3) reduces to $K \propto (9p_{12k} + 3\delta p_{2a})\chi_{12k}$, since in this case $\chi_{12k} = \chi_{2a} = \chi_{\text{slab}}/(6p_{12k} + p_{2a})$. The $T$-dependence of the shift is then completely determined by the $(\varepsilon, J)$ pair of values, whatever the value of $\delta$. When $\varepsilon > \varepsilon_0$, we recover the monotonic increase in $\delta$. Also of interest is the slow monotonic decrease of $J$ with increasing $\varepsilon$. Since $0 < J' < J$, i.e., $0 < \varepsilon < 1$, we conclude that 80 K $\lesssim J \lesssim$ 100 K. However, only the set of values for which $\delta > 1$ bear a physical solution. Two possibilities remain: (*i*) the set of values close to $\varepsilon \approx \varepsilon_0$ and (*ii*) the set of values for $\varepsilon \gtrsim 4$. Case (*ii*) is a nonphysical solution. This leads us to one of our major findings: the high-$T$ linear behavior of $K^{-1}$ reflects the physics of a pyrochlore slab, with the consequence that $K \propto \chi_{\text{slab}}$.

Results for all samples are presented in Table 1. Errors are governed by error bars on $p_{12k}$ and $p_{2a}$ from neutron diffraction data. Coupling constants are found independent on lattice coverage given the negligeable variation of lattice parameters with substitution. Turning to the value of $J$, it is very satisfying to find a coupling constant close to the one observed in $Cr_2O_3$, where $Cr^{3+}$ ions have a local octahedral

**Table 1.** Nominal occupation of Cr sites and occupations of Cr($12k$), Cr($2a$), and Cr($4f_{vi}$) sites from neutron refinement. $J$ and $\varepsilon$ are the couplings extracted from the high-$T$ mean-field analysis for the three samples.

| $p$ | $p_{12k}$ | $p_{2a}$ | $p_{4f_{vi}}$ | $J$ (K) | $\varepsilon$ |
|---|---|---|---|---|---|
| 0.81(1) | 0.79(1) | 0.95(2) | 0.81(1) | 94(9) | 0.82(2) |
| 0.89(1) | 0.89(1) | 0.94(2) | 0.86(1) | 85(6) | 0.81(2) |
| 0.96(1) | 0.96(1) | 1.00(2) | 0.94(1) | 86(6) | 0.80(1) |

environment ($d_{\mathrm{Cr-Cr}} = 2.890$ Å, Cr–O–Cr = 93.1°) similar to Cr($12k$) ($d_{\mathrm{Cr-Cr}} = 2.895$ Å, Cr–O–Cr = 93.8°). There it was established that the exchange coupling between neighboring Cr is 77(3) K [11]. We also performed a consistency test by calculating the expected values of $\Theta_{\mathrm{NMR}}$ using results reported in Table 1. The analytical expression of $\Theta_{\mathrm{NMR}}$ is obtained from the high-$T$ limit ($T >> S(S+1)J$) of expression (3). We find 456(56), 460(33), and 495(35) K for $p = 0.81$, 0.89, and 0.96, respectively, in agreement with experimental values of $\Theta_{\mathrm{NMR}}$. Finally, by using the susceptibility of Cr($4f_{vi}$)−Cr($4f_{vi}$) pairs [3], we are able to reproduce the high-$T$ $\chi_{\mathrm{macro}}$-data where the susceptibility $\chi_{\mathrm{slab}}$ adds on to the Cr($4f_{vi}$) and to the defect induced susceptibilities.

In conclusion, we have provided evidence that the Curie–Weiss behavior of the frustrated slab susceptibility extends to much lower temperatures than the average Cr–Cr interaction. A high-$T$ mean-field analysis allowed us to determine couplings involved in the frustrated physics. We confirm the common belief that frustration in SCGO($p$) arises from a pyrochlore slab.

## Acknowledgements

We acknowledge fruitful discussions with A. Keren, C. Lhuillier, F. Mila, M. Horvatić, and B. Douçot.

## References

1. P. Schiffer and A.P. Ramirez. Comments Condens. Matter Phys. **18**, 21 (1996) and references therein.
2. C. Broholm, G. Aeppli, G.P. Espinosa, and A.S. Cooper. Phys. Rev. Lett. **65**, 3173 (1990); C. Mondelli, K. Andersen, H. Mutka, C. Payen, and B. Frick. Physica B, **267/268,** 139 (1999).
3. S.-H. Lee, C. Broholm, G. Aeppli, T.G. Perring, B. Hessen, and A. Taylor. Phys. Rev. Lett. **76**, 4424 (1996).
4. P. Schiffer and I. Daruka. Phys. Rev. B: Condens. Matter Mater. Phys. **56**, 13 712 (1997).
5. P. Mendels, A. Keren, L. Limot, M. Mekata, G. Collin, and M. Horvatić. Phys. Rev. Lett. **85**, 3496 (2000).
6. A.P. Ramirez, G.P. Espinosa, and A.S. Cooper. Phys. Rev. Lett. **64**, 2070 (1990); B. Martinez, F. Sandiamenge, A. Rouco, A. Labarta, J. Rodríguez-Carvajal, M. Tovar, M.T. Causa, and X. Obradors. Phys. Rev. B: Condens. Matter Mater. Phys. **46**, 10 786 (1992).
7. A. Keren, P. Mendels, M. Horvatić, F. Ferrer, Y.J. Uemura, M. Mekata, and T. Asano. Phys. Rev. B: Condens. Matter Mater. Phys. **57**, 10 745 (1998).
8. W.G. Clark, M.E. Hanson, and F. Lefloch. Rev. Sci. Instrum. **66**, 2453 (1995).
9. K. Motida and S. Miahara. J. Phys. Soc. Jpn. **33**, 687 (1972).
10. H. Ohta, M. Sumikawa, M. Motokawa, and H. Nagasawa. J. Phys. Soc. Jpn. **65**, 848 (1996).
11. E.J. Samuelsen, M.T. Hutchings, and G. Shirane. Physica, **48**, 13 (1970).